JOURNAL OF COMPUTATIONAL PHYSICS 34, 124–135 (1980)

Note

On the Numerical Generation of Boundary-Fitted Orthogonal Curvilinear Coordinate Systems*

INTRODUCTION

A recent series of papers by Thompson *et al.* [1–3] has presented a powerful technique for the numerical generation of boundary-fitted curvilinear coordinate systems. Their technique is based on the numerical solution of coupled second-order partial differential equations, subject to some arbitrary specification of ξ around the boundary (in the notation of [1–3], which is used throughout this note). But because the differential equations are determined independently of the ξ boundary conditions, the generated coordinate system is not, is general, orthogonal.

For some applications it is more desirable to have an orthogonal coordinate system than to have a predetermined spacing of the ξ coordinate lines around the boundary. Consider, for example, the evaluation of the outward normal derivative of an arbitrary function f at the boundary of the region of interest. If the boundary is a line of constant η, then

$$\frac{\partial f}{\partial n} = \hat{n} \cdot \nabla f = \frac{1}{h_{\eta\eta}} \frac{\partial f}{\partial \eta} - \frac{(x_\xi x_\eta + y_\xi y_\eta)}{(x_\xi^2 + y_\xi^2)^{1/2} (x_\eta^2 + y_\eta^2)^{1/2}} \frac{1}{h_{\xi\xi}} \frac{\partial f}{\partial \xi}, \tag{1}$$

where $\hat{n}$ is the outward unit normal, $h_{\xi\xi}$ and $h_{\eta\eta}$ are the scale factors of the (x, y) to (ξ, η) transformation,

$$h_{\xi\xi} = (\xi_x^2 + \xi_y^2)^{-1/2} = J(x_\eta^2 + y_\eta^2)^{-1/2},$$
$$h_{\eta\eta} = (\eta_x^2 + \eta_y^2)^{-1/2} = J(x_\xi^2 + y_\xi^2)^{-1/2},$$

and $J = x_\xi y_\eta - x_\eta y_\xi$ is the Jacobian of the transformation.

If the ξ–η coordinates are orthogonal, Eq. (1) reduces to just

$$\frac{\partial f}{\partial n} = \frac{1}{h_\eta} \frac{\partial f}{\partial \eta}. \tag{2}$$

The scale factor notation can be simplified as shown since $h_{\xi\eta} = h_{\eta\xi} = 0$ for orthogonal systems, and there is no ambiguity in the use of a single subscript.

Obviously, Eq. (2) is much simpler than Eq. (1), and is to be preferred for most analytical purposes. Less obviously, but of importance to numerical schemes, Eq. (1)

* Contribution No. 381 from the NOAA/ERL Pacific Marine Environmental Laboratory.

0021-9991/80/010124–12$02.00/0

couples the ξ and η variations of the function f. Thus the application of a boundary condition on f may involve the difference of two large numbers, with a possible loss of numerical precision.

The desirability of using orthogonal curvilinear coordinates has been appreciated by past authors. Reid *et al.* [4] have employed orthogonal coordinates in storm surge simulations. Their orthogonal curvilinear coordinate system was obtained by representing the transformation as a truncated Fourier series with complex argument $w = \xi + i\eta$. Since their functional series is everywhere analytic, the real and imaginary parts of the expansion form conjugate harmonic pairs, and the transformation is conformal. They are thereby guaranteed an orthogonal mesh. The coefficients of their series were determined by a least-squares procedure in which the coastal and seaward boundaries were fit to η coordinate lines. They subsequently employed a second transformation to stretch and pack their grid for greater resolution in key areas.

The method of Reid *et al.* is fundamentally analytic. If the coordinates are not stretched, then their procedure approximates the correct transformation with an error determined by the number of terms used in the Fourier series. However, if the coordinates are subsequently stretched, then the new coordinates do not satisfy a least-squares error criterion because the final set of coordinates is not determined simultaneously. This feature is undesirable.

Pope [5] also generated orthogonal, boundary-fitted coordinates for use in fluid flow problems. He began by formulating a very general problem, but he then restricted his solution to a class of transformations that corresponds to a uniform stretching of one of the conjugate pair variables. Unlike the method of Reid *et al.*, Pope's method is fundamentally numerical. Pope alluded to the problem of the dependence of the transformation on the x–y and ξ–η domains. We shall further discuss this matter in the section on the conformal module. Although Pope's stretching allows some concentration of coordinates in a user-selected direction, it is not an ideal method for modeling mixed boundary layer and potential flow regions.

This note shows that for certain geometries the numerical method of Thompson *et al.*, can be modified so that orthogonal coordinates are generated. The properties of conformal transformations are used to outline the constraints on the method, but the final numerical procedure explicitly incorporates general stretching transformations. The solution technique, therefore, considers all coordinates simultaneously. This note can thus be regarded as a generalization of the methods of both Pope and Thompson *et al.*

Theory

Following Thompson *et al.*, ξ and η are required to satisfy Laplace' equation in the x–y plane:

$$\begin{aligned} \nabla^2\xi &= 0, \\ \nabla^2\eta &= 0. \end{aligned} \tag{3}$$

The essence of the method is that the inverse problem for x and y is now posed based on Eq. (3) and the boundary conditions, and a numerical solution is found. This idea is not original with Thompson *et al.* Winslow [6] and Chu [7] used Eq. (3) to generate boundary-fitted coordinates, which then were used to define a triangle mesh. They did not consider the possibility of generating orthogonal coordinates, since a triangle mesh excludes orthogonality of the coordinate lines.

Our development begins with the requirement that ξ and η be a conjugate harmonic pair, thereby causing the ξ–η contours to be orthogonal. The condition for ξ and η to form a conjugate harmonic pair is that they satisfy the Cauchy–Riemann equations

$$\begin{aligned} \xi_x &= \eta_y, \\ \xi_y &= -\eta_x. \end{aligned} \tag{4}$$

The Cauchy–Riemann equations imply that the scale factors of the transformation, h_ξ and h_η, satisfy $h_\xi = h_\eta = J^{1/2}$. A consequence of this equality of scale factors is that distances in the physical plane corresponding to equal increments of ξ and η are locally equal. For many applications, such as those involving boundary layers, this equality is undesirable because gradients in one direction may differ greatly in magnitude from gradients in another direction. Pope formulated constraints similar to Eq. (4), but he required the ratio of the scale factors to be a constant throughout the grid. In either case, the transformation is too constrained to be a general technique.

If two variables χ and ζ are defined as monotonic functions of ξ and η, respectively, then a countour of constant χ is parallel in the x–y plane to its corresponding ξ contour, and likewise for the ζ and η contours. Thus χ and ζ are mutually orthogonal, but their scale factors can be adjusted through the choice of the transformations, thereby providing any desired packing of the χ–ζ coordinate lines.

For convenience of notation, let ξ and η be written as monotonically increasing functions of χ and ζ, respectively,

$$\begin{aligned} \xi &= f(\chi), \\ \eta &= g(\zeta); \end{aligned} \tag{5}$$

then it is readily seen that χ and ζ retain orthogonality. Use of (5) in (3) gives

$$\begin{aligned} \nabla^2\chi &= -\frac{f''}{f'}\nabla\chi\cdot\nabla\chi, \\ \nabla^2\zeta &= -\frac{g''}{g'}\nabla\zeta\cdot\nabla\zeta, \end{aligned} \tag{6}$$

where $f' \equiv df/d\chi, f'' \equiv d^2f/d\chi^2$, etc., and $f' \neq 0$, $g' \neq 0$.

The Cauchy–Riemann equations imply

$$\chi_x = \frac{g'}{f'}\,\zeta_y$$

and

$$\chi_y = -\frac{g'}{f'}\,\zeta_x . \tag{7}$$

The independent variables must now be interchanged and the inverse problem formulated based on Eqs. (6) and (7). The transformed Cauchy–Riemann conditions (7), treating x and y as dependent variables and χ and ζ as independent variables, become

$$\begin{aligned} y_\zeta &= \frac{g'}{f'}\,x_\chi , \\ x_\zeta &= -\frac{g'}{f'}\,y_\chi . \end{aligned} \tag{8}$$

Transforming (6) and applying (7) yields

$$\mathscr{L}(x) = 0, \tag{9a}$$

$$\mathscr{L}(y) = 0, \tag{9b}$$

where

$$\mathscr{L} = \frac{\partial^2}{\partial\chi^2} + \delta^2\frac{\partial^2}{\partial\zeta^2} - F\frac{\partial}{\partial\chi} - \delta^2 G\frac{\partial}{\partial\zeta}$$

and

$$\delta(\chi, \zeta) = \frac{f'(\chi)}{g'(\zeta)}, \qquad F(\chi) = \frac{f''(\chi)}{f'(\chi)}, \qquad G(\zeta) = \frac{g''(\zeta)}{g'(\zeta)} .$$

It is to be noted that the equation for x does not explicitly depend upon y, and vice versa. However, the solutions for x and y are coupled through the application of the boundary conditions.

Boundary Conditions

Equation (9) was developed under the requirement that the Cauchy–Riemann equations hold in the interior; by implication, they must also hold on the boundaries. If, for example, a Dirichlet boundary condition for y is applied on one segment of the ζ boundary, then y_χ and thus x_ζ are known, so that a Neumann condition on x must be imposed along the same boundary. This linkage provides the coupling between the x and y solutions.

The technique is most easily explained through the use of a specific example. Figure 1 shows a geometry which might arise in the study of a free-surface wave. The values of x on the lateral boundaries and the values of y on the bottom and surface are specified and result in Dirichlet conditions. Complementary Neumann conditions for

x on the bottom and surface and for y on the sides are obtained from the Cauchy–Riemann equations (8). Thus on the bottom and surface x is required to satisfy

$$x_\zeta = -\frac{g'}{f'} y_x ,$$

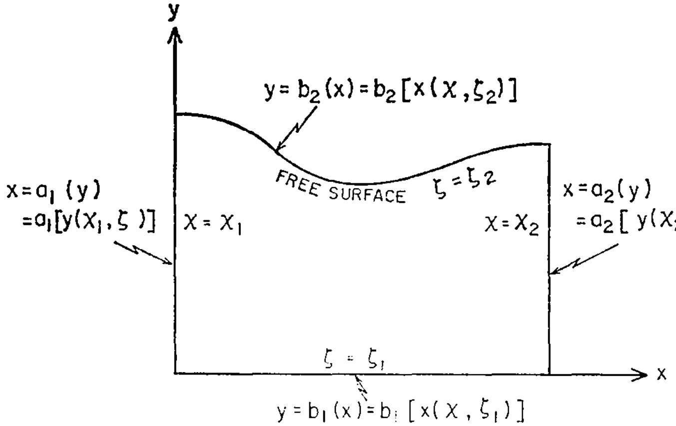

FIG. 1. Example of geometry of a free-surface wave in the physical plane.

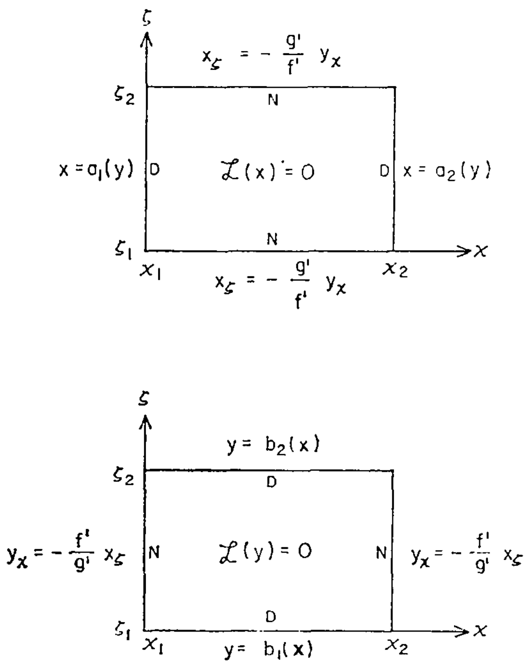

FIG. 2. Boundary conditions for x and y in the transformed plane. D and N denote Dirichlet and Neumann conditions, respectively.

and on the sides y must satisfy

$$y_\chi = -\frac{f'}{g'} x_\zeta .$$

These equations are simultaneous in nature, since y is known only as a function of x, and not as a function of χ, at the surface and bottom. Figure 2 shows the boundary conditions in the transformed plane.

The Conformal Module

A rather subtle constraint on the transformation from the physical plane P (Fig. 1) to the transformed plane T (Fig. 2) remains to be discussed. For simplicity consider the case of no coordinate stretching, $\xi = \chi$ and $\eta = \zeta$, so that the transformation is conformal. Figure 2 shows that the curvilinear quadrilateral of Fig. 1 is to be mapped onto a rectangle of length $\xi_2 - \xi_1$ and width $\eta_2 - \eta_1$. The Riemann Mapping Theorem guarantees that any simply connected domain with more than one boundary point can be conformally mapped onto any other simply connected domain with more than one boundary point. This theorem does not, however, give any information about the relation between the boundary points of the domains. In order for the transformation to be useful, it is necessary that the corner points of the physical domain P transform to the corner points of the transformed rectangle T.

Corner points of P map to corner points of T if and only if the conformal modules of the two regions are equal [8]. The conformal module of a rectangle is by definition the ratio of its length to its width; thus the module of the transformed region T is just $m(T) = (\xi_2 - \xi_1)/(\eta_2 - \eta_1)$. For convenience in labeling an $M \times N$ finite-difference grid, it would be desirable if ξ and η could be chosen such that $\xi_1 = 1$, $\xi_2 = M$, $\eta_1 = 1$, and $\eta_2 = N$. But such an arbitrary choice is not possible if the transformation is to remain conformal, since $m(T)$ must equal $m(P)$. However, if a linear scaling of ξ is made, so that $\xi = S\chi$ and $\eta = \zeta$, then χ and ζ can be chosen as desired (i.e., $\chi_1 = 1$, $\chi_2 = M$, etc.). The constant S is related to $m(P)$ by

$$m(P) = \frac{\xi_2 - \xi_1}{\eta_2 - \eta_1} = \frac{S(M-1)}{N-1} . \tag{10}$$

For the simple geometry of Fig. 1, $m(P)$ can be determined analytically, as in shown in the Appendix. However, the determination of the conformal module $m(P)$ for an arbitrary region is a difficult task. Therefore it is desirable to have a numerical procedure for determining S.

Clearly, if, for example, the solution for $y(\chi, \zeta)$ were known, then the transformed Cauchy–Riemann equation

$$\frac{1}{S}\frac{\partial x}{\partial \chi} = \frac{\partial y}{\partial \zeta}$$

could be integrated along a line of constant ζ to give

$$\frac{1}{S}\int_{\chi_1=1}^{\chi_2=M} \frac{\partial x}{\partial \chi}\, d\chi = \int_1^M \frac{\partial y}{\partial \zeta}\, d\chi$$

or

$$S = [x(M) - x(1)] \Big/ \int \frac{\partial y}{\partial \zeta}\, d\chi. \tag{11}$$

This same relationship was used by Pope to determine the scale factor in his grid generation procedure. His derivation was based on a general condition for orthogonality, and he did not discuss the connection between the scaling constant S and the conformal module $m(P)$.

Of course, Eq. (11) cannot be used unless y is known. We find, however, as did Pope, that if S is recomputed at each iteration as the numerical solution for y is iteratively generated, then convergence is rapid and the results are in agreement with those obtained if the analytical form for $m(P)$ is used to determine S.

In terms of the stretched χ–ζ coordinates, the above constraints on the transformation require only that the stretching functions $\xi = f(\chi)$ and $\eta = g(\zeta)$ be chosen such that $f(\chi) = Sf_0(\chi)$, where $f_0(\chi)$ and $g(\zeta)$ are chosen so that

$$\begin{aligned} f_0(\chi_1) &= \chi_1 = 1, \\ f_0(\chi_2) &= \chi_2 = M, \\ g(\zeta_1) &= \zeta_1 = 1, \\ g(\zeta_2) &= \zeta_2 = N. \end{aligned}$$

The numerical grid then has $M - 1$ by $N - 1$ cells, with $\Delta\chi = \Delta\zeta = 1$.

Solution Technique

Equations (9a) and (9b), including the scale factor S, can be solved by using successive overrelaxation. Sweeps are made through the χ–ζ grid, with x being updated on one sweep and y being updated on the next. The given Dirichlet conditions are linearly interpolated to generate initial guesses for x and y.

As alternating sweeps on x and y are made, the x and y values associated with a particular boundary χ–ζ grid point change on those boundaries where Neumann conditions are specified. The most recent y values at the grid points of the surface and bottom boundaries are used in computing x_ζ for updating x on these boundaries. Then these updated x values are used to compute new y values for these boundary grid points; these new y values become the Dirichlet conditions for y when the next sweep through the grid is made to update y. This shows the manner in which the solutions of x and y are coupled through the boundary conditions. After each sweep on x and y, the value of S is updated using Eq. (11).

Results

Figures 3–6 show several orthogonal grids generated by the above technique. Table I shows the packing functions f_0 and g used for these figures. The functional forms of f_0 and g were chosen to give packing in the desired areas. The value $a = 0.95$ in Table I was chosen to give the desired intensity of packing. In all cases the χ lines are labeled from 1 to M and the ζ lines are labeled from 1 to N, for an $M \times N$ grid. The coordinate lines are orthogonal to better than 0.1° on the average, and to within 1.0° at the worst locations.

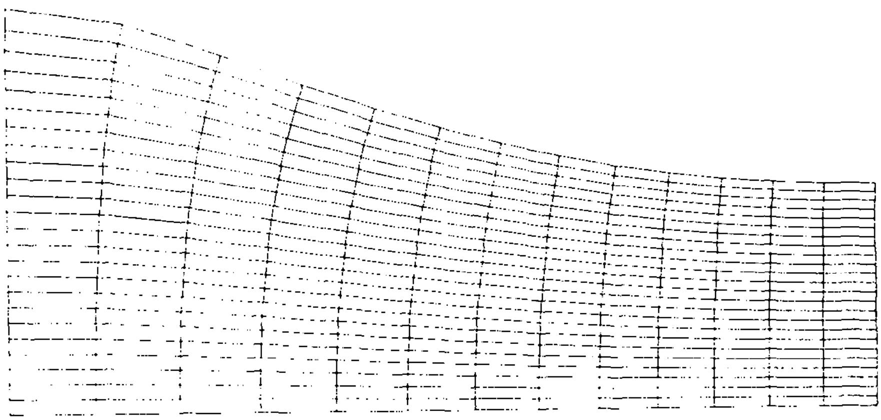

FIG. 3. Stoke's fourth-order surface profile with no packing of the grid lines.

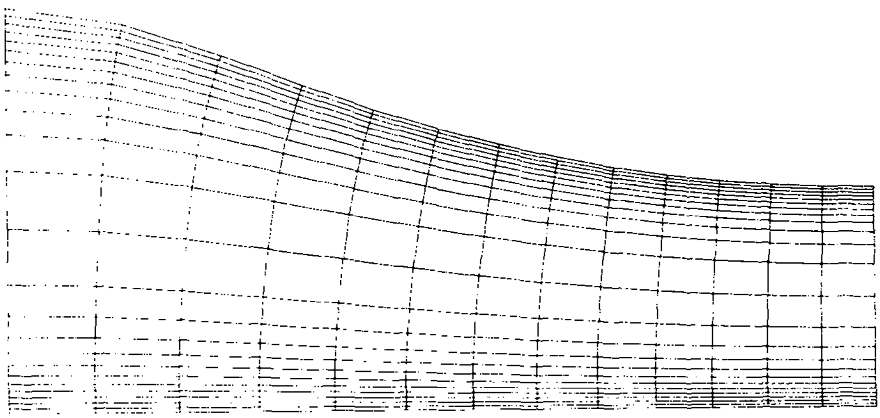

FIG. 4. Stoke's fourth-order surface profile with packing of the grid lines to the surface and bottom boundaries.

Once the grid has been obtained, i.e., once $x(\chi, \zeta)$ and $y(\chi, \zeta)$ are known, the solution of the problem at hand proceeds in the χ–ζ plane just as in the case of a non-orthogonal grid, with, of course, those simplifications that result from the orthogonality of χ and ζ.

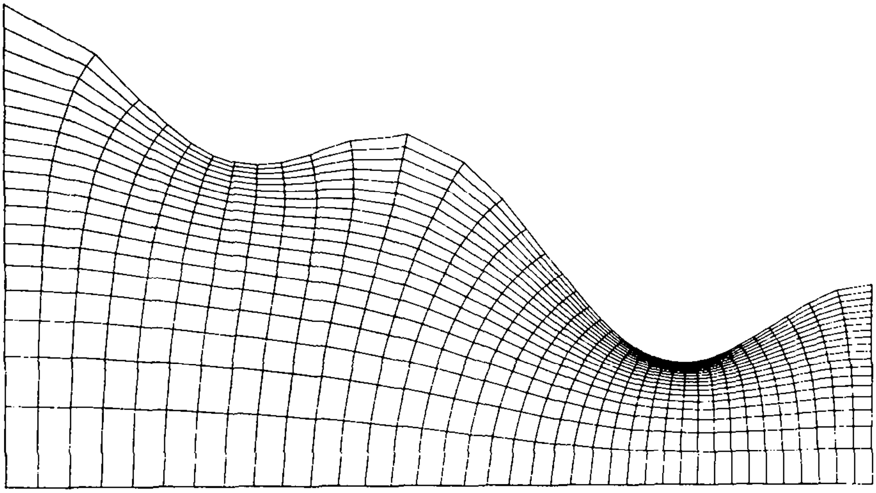

FIG. 5. Modulated cosine profile with packing of the coordinate lines near the surface.

TABLE I

The Packing Functions $\xi = f_0(\chi)$ and $\eta = g(\zeta)$ used to generate Figs. 3–6

Figure	Packing functions
3	$f_0(\chi) = \chi$
	$g(\zeta) = \zeta$
4	$f_0(\chi) = \chi$
	$g(\zeta) = \dfrac{N+1}{2} + \dfrac{N-1}{2\sinh^{-1}((N-1)/2)} \sinh^{-1}\left(\zeta - \dfrac{N+1}{2}\right)$
5	$f_0(\chi) = \chi$
	$g(\zeta) = \dfrac{N-1}{\ln N} \ln\left[\zeta \exp\left(\dfrac{\ln N}{N-1}\right)\right]$
6	$f_0(\chi) = \dfrac{M+1}{2} + \dfrac{M-1}{2\sin^{-1}(a)} \sin^{-1}\left[\dfrac{2a}{M-1}\left(\chi - \dfrac{M+1}{2}\right)\right]$
	$g(\zeta) = \dfrac{N-1}{\ln N} \ln\left[\zeta \exp\left(\dfrac{\ln N}{N-1}\right)\right]$

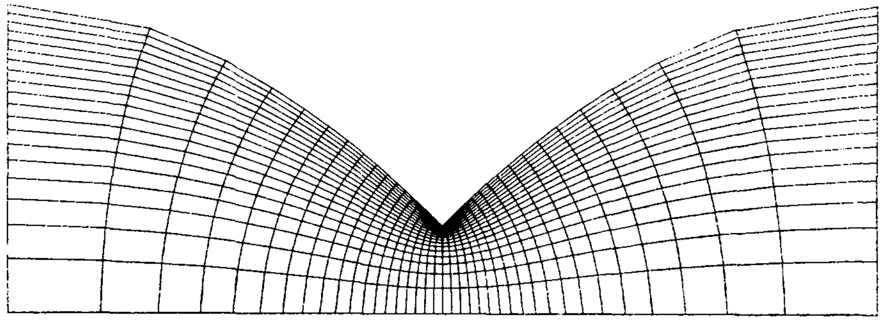

FIG. 6. Boundary cusp with both horizontal and vertical packing into the region of the cusp.

APPENDIX

No general techniques are available for the determination of the conformal module of an arbitrarily shaped region. However, the geometry of Fig. 1 can be treated by the following asymptotic method. Let the x–y axes be chosen so that the physical domain P is bounded by $x = 0$ on the left, $x = \pi$ on the right, $y = -y_B$ on the bottom, and $y = y_S(x)$ along the top (free surface), with the average surface lying at $y = 0$. Let $w = F(z)$ be the analytic transformation from the physical plane (with $z = x + iy$) to the unpacked transformed plane (with $w = \xi + i\eta$). The ξ and η axes are chosen so that the transformed domain is given by $0 \leqslant \xi \leqslant \xi_0$, $0 \leqslant \eta \leqslant \eta_0$.

With this choice of axes, the conformal module is $m(T) = \xi_0/\eta_0$. The equality of modules implies that if a value for η_0, say, is specified, then the value of ξ_0 is also fixed. By determining ξ_0 as a function of η_0 and the parameters of the physical domain, the module $m(P)$ can be determined.

$F(z)$ can be expanded as

$$w = Az + iB + i \sum_{k=1}^{\infty} [C_k \exp(-ikz) + D_k \exp(ikz)],$$

where the coefficients A, B, C_k, and D_k are all real. Equating real and imaginary components gives

$$\xi = Ax + \sum_{k=1}^{\infty} [C_k \exp(ky) - D_k \exp(-ky)] \sin(kx), \tag{A1}$$

$$\eta = Ay + B + \sum_{k=1}^{\infty} [C_k \exp(ky) + D_k \exp(-ky)] \cos(kx). \tag{A2}$$

Note that at $x = \pi$, $\xi = \xi_0 = \pi A$, so the task is reduced to determining A.

The bottom boundary condition, $\eta(x, -y_B) = 0$, gives the recursion relations

$$A y_B = B,$$
$$D_k = -C_k \exp(-2k y_B).$$

The free surface $y = y_S(x)$ can be expanded in a cosine series as

$$y_S(x) = \sum_{k=1}^{\infty} a_k \cos(kx). \tag{A3}$$

The corresponding η coordinate line, η_0, can be expanded in a Taylor's series about the average surface position, $y = 0$, as

$$\eta_0 = \eta(x, 0) + y_S \frac{\partial \eta}{\partial y}(x, 0) + \frac{1}{2} y_S{}^2 \frac{\partial^2 \eta}{\partial y^2}(x, 0) + \cdots . \tag{A4}$$

The derivatives of η in (A4) can be evaluated from (A2). Substitution of these derivatives and of (A3) into (A4) gives an expression for η_0 as a series in $\cos(kx)$, $k = 0, 1, 2,\ldots$. Since the value of η_0 is independent of x, the coefficients of $\cos(kx)$ must be zero for $k \geqslant 1$. This observation allows the determination of A to any desired accuracy by the inclusion of a sufficient number of terms in the series (A2), (A3), and (A4).

For example, retaining only terms through $k = 1$ in (A2) and (A3) and retaining only the first two terms in (A4) give the lowest-order expansion for η_0:

$$\eta_0 = [A y_B + \tfrac{1}{2} a_1 C_1 (1 + \exp(-2 y_B))] + [A a_1 + C_1 (1 - \exp(-2 y_B))] \cos(x).$$

Equating the coefficient of $\cos(x)$ to zero gives

$$A = \eta_0 [y_B - \tfrac{1}{2} a_1{}^2 \coth(y_B)]^{-1}.$$

The lowest-order approximation for the conformal module of the physical region is thus

$$m(P) = \pi A / \eta_0 = \frac{\pi}{y_B} [1 - \tfrac{1}{2} a_1{}^2 \coth(y_B)/y_B]^{-1}.$$

Acknowledgment

The authors wish to thank Dr. C. Wayne Mastin for pointing out the connection between the scale factor S and the conformal module $m(P)$. We also wish to thank Dr. Harold Mofjeld for his helpful discussion on the analytic solution to the conformal module problem.

REFERENCES

1. J. F. THOMPSON, F. C. THAMES, AND C. W. MASTIN, *J. Computational Physics* **15** (1974), 299.
2. F. C. THAMES, J. F. THOMPSON, C. W. MASTIN, AND R. L. WALKER, *J. Computational Physics* **24** (1977), 245.
3. J. F. THOMPSON, F. C. THAMES, AND C. W. MASTIN, *J. Computational Physics* **24** (1977), 274.
4. R. O. REID, A. C. VASTANO, R. E. WHITAKER, AND J. J. WANSTRATH, *in* "The Sea" (E. D. Goldberg, Ed.), Vol. 6, Chap. 5, Wiley, New York, 1977.
5. S. B. POPE, *J. Computational Physics* **26** (1978), 197.
6. A. M. WINSLOW, *J. Computational Physics* **2** (1967), 149.
7. W-H. CHU, *J. Computational Physics* **8** (1971), 392.
8. D. GAIER, *in* "Functional Analysis and Its Applications," Lecture Notes in Mathematics, No. 399, Springer-Verlag, Berlin, 1974.

RECEIVED: October 17, 1978; REVISED: May 8, 1979

CURTIS D. MOBLEY† AND ROBERT J. STEWART

National Oceanic and Atmospheric Administration
Environmental Research Laboratories
Pacific Marine Environmental Laboratory
Seattle, Washington 98105

† Research performed while a National Research Council Resident Research Associate.